Psychological Medicine

cambridge.org/psm

The prediction of resilience to alcohol consumption in youths: insular and subcallosal cingulate myeloarchitecture

Kathrin Weidacker[1,*], Seung-Goo Kim[1,2,*], Mette Buhl-Callesen[3], Mads Jensen[4], Mads Uffe Pedersen[3], Kristine Rømer Thomsen[3,*] and Valerie Voon[1,*]

[1]Department of Psychiatry, University of Cambridge, Cambridge, UK; [2]Department of Psychology and Neuroscience, Duke University, Durham, North Carolina, USA; [3]Centre for Alcohol and Drug Research, School of Business and Social Sciences, University of Aarhus, Aarhus, Denmark and [4]Center of Functionally Integrative Neuroscience, MINDLab, Aarhus University, Aarhus, Denmark

Original Article

*These authors contributed equally to the study.

Cite this article: Weidacker K, Kim S-G, Buhl-Callesen M, Jensen M, Pedersen MU, Thomsen KR, Voon V (2020). The prediction of resilience to alcohol consumption in youths: insular and subcallosal cingulate myeloarchitecture. *Psychological Medicine* 1–11. https://doi.org/10.1017/S0033291720003852

Received: 22 May 2019
Revised: 7 March 2020
Accepted: 26 September 2020

Key words:
adolescent; alcohol consumption; insula; longitudinal relaxation rate; myeloarchitecture; resilience; subcallosal cingulate

Author for correspondence:
Valerie Voon, E-mail: vv247@cam.ac.uk

Abstract

Background. The prediction of alcohol consumption in youths and particularly biomarkers of resilience, is critical for early intervention to reduce the risk of subsequent harmful alcohol use.

Methods. At baseline, the longitudinal relaxation rate (R1), indexing grey matter myelination (i.e. myeloarchitecture), was assessed in 86 adolescents/young adults (mean age = 21.76, range: 15.75–26.67 years). The Alcohol Use Disorder Identification Test (AUDIT) was assessed at baseline, 1- and 2-year follow-ups (12- and 24-months post-baseline). We used a whole brain data-driven approach controlled for age, gender, impulsivity and other substance and behavioural addiction measures, such as problematic cannabis use, drug use-related problems, internet gaming, pornography use, binge eating, and levels of externalization, to predict the change in AUDIT scores from R1.

Results. Greater baseline bilateral anterior insular and subcallosal cingulate R1 (cluster-corrected family-wise error $p < 0.05$) predict a lower risk for harmful alcohol use (measured as a reduction in AUDIT scores) at 2-year follow-up. Control analyses show that other grey matter measures (local volume or fractional anisotropy) did not reveal such an association. An atlas-based machine learning approach further confirms the findings.

Conclusions. The insula is critically involved in predictive coding of autonomic function relevant to subjective alcohol cue/craving states and risky decision-making processes. The subcallosal cingulate is an essential node underlying emotion regulation and involved in negative emotionality addiction theories. Our findings highlight insular and cingulate myeloarchitecture as a potential protective biomarker that predicts resilience to alcohol misuse in youths, providing novel identifiers for early intervention.

Introduction

Alcohol misuse is a major international public health issue with high morbidity and mortality and marked costs. Alcohol use is particularly common in youths, about 26.5% of 15–19-year olds are current drinkers (World Health Organization, 2018), an age range that coincides with high neurodevelopmental vulnerability. Globally, 3 million people per year die due to excessive alcohol consumption (5.3% of all deaths per year), with an even higher rate of 13.5% in young adults, aged between 20 and 39 years (World Health Organization, 2018). While alcohol usage usually starts at an early age, before the age of 15, the earlier the age of alcohol use onset, the greater the risk of subsequent alcohol use disorders (Behrendt, Wittchen, Höfler, Lieb, & Beesdo, 2009; World Health Organization, 2018). Thus, the identification of biomarkers, a measured variable that relates to the disease (Ballman, 2015), which identifies youths at risk for problematic alcohol use is critical for the development of early intervention programmes.

Functional and structural imaging studies have focused on such predictive biomarkers in youths. For instance, Dager et al. (2014) identified college students (18–21 years old) transitioning from moderate to heavy drinking over the course of 1 year and students with stable drinking behaviour via online monthly substance use surveys that assessed the number of drinking days, binge drinking and typical and maximum number of drinks in the previous months. Comparing these student groups on their baseline neural activity to pictures of alcoholic *v.* non-alcoholic beverages revealed higher activity in transitioners in insular, ventromedial prefrontal cortex, anterior cingulate cortex (ACC), orbitofrontal cortex and caudate (Dager et al., 2014). Similarly, a large multicentre study in 14-year olds assessed alcohol usage via the Alcohol Use Disorder Identification Test (AUDIT; Saunders, Aasland, Babor,

CAMBRIDGE UNIVERSITY PRESS

De la Fuente, & Grant, 1993) to identify youths with low/medium levels of pre-existing alcohol problems. Applying structural equation modelling to this cohort, an early onset of alcohol consumption was predicted by greater neural activity during the anticipation of large when compared to that of small rewards in the striatum, prefrontal areas, insula and amygdala (Nees et al., 2012). In the same cohort, machine learning was applied to predict future binge drinking from structural abnormalities measured by grey matter volume (GMV) and from neural activity during stop signal trials of failed motor inhibition (*v.* implicit baseline). This investigation revealed early abnormalities predicting future binge drinking behaviour in the GMV and brain activity in parahippocampal and postcentral gyri (Whelan et al., 2014).

While measures of neural activity and GMV are informaptive of pre-existing abnormalities, measures of myeloarchitecture (microarchitecture of myelinated axons in grey matter) may be particularly relevant to behavioural outcomes (see Edwards, Kirilina, Mohammadi, & Weiskopf, 2018). The quantification of myeloarchitecture can include approaches such as T1-weighted and T2-weighted image intensity ratios, magnetization transfer (MT) mapping, and longitudinal relaxation time (T1) mapping, which has been identified as the best approach to map *in vivo* myelin distribution in the cortical and subcortical grey matter (Haast, Ivanov, Formisano, & Uludag, 2016). Longitudinal relaxation rate (R1 = 1/T1) is sensitive to age-related effects with increasing frontal and parietal and decreasing optic radiation and corpus callosal indices with age (Callaghan et al., 2014) and might therefore be a useful measure for structural integrity in adolescence. R1 has also been found sensitive to pathological abnormalities, disorders such as major depression have been associated with a wide-spread reduction in left dorsolateral prefrontal R1, a measure also associated with a greater number of depressive episodes (Sacchet & Gotlib, 2017). Additionally, R1 quantification has also been linked to cognitive function: Musicians with greater capacity to recognize and label pitch chroma without references have greater auditory R1 (Kim & Knoesche, 2016) and inferior parietal R1 has been associated with greater empathic traits (Allen et al., 2017). Moreover, we recently showed that R1 in the ventral putamen is negatively correlated with a form of impulsivity characterized by premature or early responding (Nord et al., 2019). More recently, a reduced growth of grey matter myelination, measured by MT imaging, in lateral and medial prefrontal regions was associated with impulsivity in an adolescent healthy population (Ziegler et al., 2019). Importantly, increased impulsivity levels are a common feature in substance abuse (Rømer Thomsen et al., 2018) and therefore hint towards a role for R1 in predicting future substance use. Additional support for the hypothesis that R1 plays a role in alcohol addiction stems from related structural measures of brain integrity. For example, GMV, as estimated by Jacobian-modulated grey matter probabilities, has been found to relate to craving and were reduced in alcohol dependence (Senatorov et al., 2015). Since the GMV could be affected by local myelin density of a grey matter voxel (which increases T1-weighted image intensity, thus reduces grey matter probability), this finding provides evidence for structural abnormalities where assessing R1 would further clarify whether myelination density in grey matter is the underlying source of structural abnormalities.

However, to the best of our knowledge, R1 has not yet been utilized in terms of addiction. Here we, therefore, assess the role of structural imaging measures using a data-driven, exploratory, approach in predicting subsequent resilience to alcohol mis/use in youths. We assess R1 of grey matter at baseline and measures of substance and behavioural addiction at baseline, 1- and 2-year follow-up in youths (Rømer Thomsen et al., 2013). To show the unique sensitivity of R1, we additionally test associations between other structural measures (local volume and fractional anisotropy) of grey matter and behavioural measure changes. Although most research has focused on risk factors for the development of problem behaviours (Hawkins, Catalano, & Miller, 1992; Hodder et al., 2018; Scheier, Botvin, & Baker, 1997), not all adolescents who use substances develop problematic behaviours. As our sample largely decreased their use of alcohol over time, we thus address a critical question of resilience or protective factors.

Methods and materials

Participants

Participants were selected from a representative national survey (*YouthMap2014 by Statistics Denmark*, $n = 3064$) based on their level of externalizing problems (EP) assessed using YouthMap12 (Pedersen, Rømer Thomsen, Pedersen, & Hesse, 2017). See online Supplementary materials for details. Participants were instructed to abstain from substances at least 24 h prior to participation. The study was approved by the local ethics committee and consent was obtained from the participant or their parents if the participant was under 18.

In total, 103 participants were invited to CFIN/MINDLab facilities at Aarhus University, Denmark to complete computerized questionnaires, behavioural tests and MRI scanning at baseline, and questionnaires 3 times over 2 years (91.3% participated at 1-year follow-up; 83.5% participated at 2-year follow-up). The follow-up sessions were spaced by 12 and 24 months, respectively.

For the 86 subject who participated in all sessions, baseline neuroimaging data and behavioural measures up to the second follow-up were analysed in the current study. The age of the analysed subjects at baseline ranged between 15.8 and 26.7 years ($M = 21.8$, S.D. = 2.8) with 32.6% female.

Self-report measures of addictive behaviours

Problematic alcohol use was measured using the AUDIT (Saunders et al., 1993), a 10-item questionnaire validated as a screening instrument for hazardous and harmful alcohol use with good sensitivity and specificity. To enable statistical corrections for other substance and behavioural addiction measures, the following instruments were used at baseline: Cannabis Use Disorder Identification Test-Revised (CUDIT-R; Adamson & Sellman, 2003), Drug Use Disorder Identification Test (DUDIT; Berman, Bergman, Palmstierna, and Schlyter, 2005), Internet Gaming Disorder Scale Short Format (IGD; Pontes & Griffiths, 2015), Pornography Craving Questionnaire, (PCQ; Kraus & Rosenberg, 2014) and Binge Eating Scale (BES; Gormally, Black, Daston, and Rardin, 1982). See online Supplementary Methods for details. Correlations between self-reported addictive behaviours are shown in online Supplementary Table S1. The change in AUDIT score did not correlate with changes in other substance or behavioural addiction measures. Impulsivity traits were measured using the UPPS-P Impulsive Behaviour Scale (Cyders et al., 2007; Lynam, Smith, Whiteside, & Cyders, 2006).

Imaging acquisition

At baseline, MP2RAGE (Marques et al., 2010) images were acquired using Siemens Skyra 3-Tesla MR system with following

parameter: TE (echo time) = 2.98 ms, TI1 (first inversion time) = 700 ms, TI2 (second inversion time) = 2500 ms, FA1 (first flip angle) = 4°, FA2 (second flip angle) = 5°, TR (time of repetition) = 5000 ms, voxel size = $1 \times 1 \times 1$ mm^3. The MP2RAGE sequence acquires two inversion images with different flip angles and inversion times (unlike the conventional MPRAGE sequence) and derives a T1 image and a uniform tissue-contrast image (Marques et al., 2010). While the MP2RAGE sequence was initially motivated to estimate unbiased tissue-contrast, it provides a good estimation of T1, which is mainly influenced by the myelin concentration (Rooney et al., 2007; Stüber et al., 2014). Note that here 'T1 images' are in a physical scale of time (i.e. sec) as they are the estimation of longitudinal relaxation time (T1) whereas 'T1-weighted images' are in an arbitrary scale as at they are relative MR signal at the time when the contrast between grey and white matter in the longitudinal magnetization is optimized. We note that no additional imaging data were acquired at follow-up sessions.

Image processing

Uniform-contrast (i.e. T1-weighted-like) images were segmented and spatially normalized using unified segmentation (Ashburner & Friston, 2005) in SPM12 (7219; https://www.fil.ion.ucl.ac.uk/spm/). To confine the analysis to grey matter, the longitudinal relaxation rate (R1 = 1/T1; positively correlates with myelin content) images were masked by grey matter masks in native space, then non-linearly transformed into the Montreal Neurological Institute (MNI) template space using the deformation field from the unified segmentation, resampled at 1.5 mm isotropic resolution. Spatial smoothing with a 3-D isotropic Gaussian kernel with the full-width at half-maximum (FWHM) of 6 mm was applied.

General linear model for neuro-behaviour association

We tested the behavioural and demographic parameters for normality (Shapiro–Wilkes test), skewness and outliers prior to using the general linear model (GLM). We used parametric tests as R1 residuals were consistent with Gaussian distribution (Lilliefors test, $p > 0.15$, FDR-corrected). There was no multicollinearity detected among all regressors in the GLM (online Supplementary Table S3).

To assess the relationship between imaging measures collected at baseline and cross-sectional behavioural parameters, we first tested whether R1 was significantly associated with cross-sectional baseline scores covarying for age and sex (similar to GLM 4 below). There were no significant correlations with R1 and any baseline measures of substance (including AUDIT) or behavioural addiction (uncorrected $p > 0.07$).

Then we tested the association between R1 and longitudinal changes in AUDIT using the following GLM:

$$R1 = \beta_0 + \beta_1 \Delta\mathrm{AUDIT}_{k-0} + \varepsilon, \quad (1)$$

where $\Delta\mathrm{AUDIT}_{k-0}$ is a difference between the k-th (either the first or second) follow-up measurement and the baseline (the zeroth) measurement of AUDIT, and ε is a zero-mean unit-variance Gaussian error. The significance of the association between R1 and $\Delta\mathrm{AUDIT}_{k-0}$ was tested using T-contrasts [$T = \hat{\beta}.c'/\sqrt{\hat{\sigma}^2 c'(M'M)^{-1}c}$ where the contrast vector c is (0 1) or (0–1), $\hat{\sigma}^2$ is a sample variance, and $\mathbf{M}$ is a design matrix].

Since sex and age covary with R1 (Edwards et al., 2018; Keuken et al., 2017; Kim & Knoesche, 2016), we tested these effects for significance using F-contrasts (H_0:$\beta_1 = 0$ *v.* H_A:$\beta_1 \neq 0$):

$$R1 = \beta_0 + \beta_1 \mathrm{age} + \beta_2 \Delta\mathrm{AUDIT}_{k-0} + \varepsilon, \quad (2)$$

and

$$R1 = \beta_0 + \beta_1 \mathrm{sex} + \beta_2 \Delta\mathrm{AUDIT}_{k-0} + \varepsilon, \quad (3)$$

Thus, we tested whether the inclusion of a particular covariate would significantly change the ratio of explained variance. As we found significant effects of age and sex on R1 (online Supplementary Fig. S1), we covaried them both as:

$$R1 = \beta_0 + \beta_1 \mathrm{age} + \beta_2 \mathrm{sex} + \beta_3 \Delta\mathrm{AUDIT}_{k-0} + \varepsilon. \quad (4)$$

To assess for specificity for alcohol consumption among other impulsive behaviours (UPPS, other addictive measures) and control for other variables [BDI (Beck Depression Inventory)] (Sacchet & Gotlib, 2017), we compared the GLM (4) with an extended model as follows:

$$R\beta_1 \mathrm{age} + \beta_2 \mathrm{sex} + \beta_3 \Delta\mathrm{AUDIT}_{k-0} + \beta_4 X + \varepsilon. \quad (5)$$

where X is either BDI, EP, Urgency, Premeditation, Perseveration, Sensation, $\Delta\mathrm{CUDIT}_{k-0} + \Delta\mathrm{DUDIT}_{k-0} + \Delta\mathrm{IGD}_{k-0} + \Delta\mathrm{PCQ}_{k-0} + \Delta\mathrm{BES}_{k-0}$. Δx_{k-0} is a difference between the k-th (either the first or second) follow-up measurement and the baseline (the zeroth) measurement of the variable x. An F-contrast comparing two models (H_0:$\beta_4 = 0$ *v.* H_A:$\beta_4 \neq 0$) tests whether the additional term X explains residuals of a reduced model significantly or not.

Finally, we also compared GLM (4) with models with all UPPS or all addiction variables:

$$\begin{aligned} R1 =& \beta_0 + \beta_1 \mathrm{age} + \beta_2 \mathrm{sex} + \beta_3 \Delta AUDIT_{k-0} + \beta_4 \mathrm{Urgency} \\ &+ \beta_4 \mathrm{Premeditation} + \beta_4 \mathrm{Perseveration} + \beta_4 \mathrm{Sensation} + \varepsilon, \end{aligned} \quad (6)$$

and

$$\begin{aligned} R1 =& \beta_0 + \beta_1 \mathrm{age} + \beta_2 \mathrm{sex} + \beta_3 \Delta AUDIT_{k-0} + \beta_4 \Delta CUDIT_{k-0} \\ &+ \beta_4 \Delta DUDIT_{k-0} + \beta_4 \Delta IGD_{k-0} \\ &+ \beta_4 \Delta PCQ_{k-0} + \beta_4 \Delta BES_{k-0} + \varepsilon. \end{aligned} \quad (7)$$

Family-wise error rate (FWER) was controlled below 0.05 at the cluster level using Random Field Theory (Worsley, Evans, Marrett, & Neelin, 1992) implemented in SPM12. Cluster forming threshold was 0.005 and extent threshold was determined based on the data as the smallest volume of a cluster with the corrected p value <0.05, which was 490 voxels (1654 mm^3). Search space was restrained to grey matter to match processed images.

Anatomical annotation of found clusters was based on Harvard-Oxford Atlas and Talairach Daemon Atlas included in FSL (https://fsl.fmrib.ox.ac.uk). To further determine insular subregions, we also used a probabilistic atlas of the human insular cortex (Faillenot, Heckemann, Frot, & Hammers, 2017) available at http://brain-development.org/.

Relevant vector regression

We further investigated information values of R1 patterns of the regions identified from the significant linear relationships from the GLM analyses to further explore the non-linear relationship between neural and behavioural measures by using a machine learning technique called Relevant Vector Regression (RVR; Tipping, 2001). RVR decodes (or predicts) an unknown continuous target value from learnt non-linear mapping between multivariate measures and the target value (i.e. kernel) utilizing sparse Bayesian learning framework achieving comparable generalizability more efficiently than support vector machine (SVM). We used an RVR implemented in Pattern Recognition for Neuroimaging Toolbox available via http://www.mlnl.cs.ucl.ac.uk/pronto/ (Schrouff et al., 2013).

To avoid circular fallacy (Kriegeskorte, Simmons, Bellgowan, & Baker, 2009), regions of interests were picked from an independent anatomical atlas ('Hammersmith n30r95'): 'insular anterior short gyrus' and 'insular anterior inferior cortex' for insular models and 'subgenual frontal cortex' and 'subcallosal area' for a subcallosal cortical model. Similar atlas-based approaches were used in previous prediction studies on alcohol consumption (Seo et al., 2015,2019). For comparison, a whole-brain model was also constructed.

For each given region, demeaned R1 patterns of individuals were entered as multivariate inputs covaried for age and sex. Leave-one-out cross-validation (LOOCV) was performed to compute the model's prediction accuracy and examined using root mean squared error (RMSE) and prediction R^2. Significance was tested from 1000 permutations (random assignment of AUDIT changes), in which AUDIT changes were randomly permuted and LOOCV performed in each iteration.

Control analysis

In addition to R1, we also investigated local GMV (Ashburner & Friston, 2000), and fractional anisotropy (FA) based on diffusion-weighted images (Basser, Mattiello, & LeBihan, 1994). Details are explained in online Supplementary materials. In short, we did not find significant associations with the longitudinal changes of AUDIT in the baseline GMV and FA (cluster-$p > 0.85$); thus, we focused on the R1 findings in the following sections.

Results

Longitudinal changes in addictive behaviours

The demographic variables, UPPS scores, and addictive behaviours at baseline and their longitudinal changes are shown in Table 1. CUDIT, DUDIT, and IGD significantly decreased after 1 year (i.e. changes between the first follow-up and baseline (1–0)). After 2 years (i.e. changes between the second follow-up and baseline (2–0)), AUDIT and IGD significantly decreased whereas BES significantly increased.

Changes in AUDIT were negatively correlated with the baseline measure [$r(\mathrm{AUDIT}_0, \Delta\mathrm{AUDIT}_{1-0}) = -0.39$, $p = 0.0002$; r $(\mathrm{AUDIT}_0, \Delta\mathrm{ADUIT}_{2-0}) = -0.60$, $p = 10^{-9}$]. Taken together with the general decrease in AUDIT (online Supplementary Table S1), individuals who reported higher AUDIT baseline later reported decreased AUDIT in the follow-up measures (online Supplementary Fig. S2).

Correlations between grey matter myelination and AUDIT changes

We tested for correlations between baseline grey matter R1 (longitudinal relaxation rate) and AUDIT changes after 1 ($\Delta\mathrm{AUDIT}_{1-0}$) and 2 years ($\Delta\mathrm{AUDIT}_{2-0}$) and found significant correlations only with $\Delta\mathrm{AUDIT}_{2-0}$ but not $\Delta\mathrm{AUDIT}_{1-0}$ (cluster-$p > 0.05$). Thus, here we only report GLM results for the AUDIT changes after 2 years.

First in GLM (1), we found a negative correlation of the 2-year AUDIT change ($\Delta\mathrm{AUDIT}_{2-0}$) and R1 in bilateral insula (cluster-$p < 0.001$) and the ACC/subcallosal cortex (SCA; cluster-$p = 0.045$; Fig. 1*a–e* and Table 2).

As age and sex significantly increased explained variance (GLM 2, 3; cluster-$p < 0.044$), we controlled for age and sex (GLM 4): AUDIT change remained negatively associated with R1 in bilateral insula and SCA (cluster-$p < 0.034$; Fig. 1*f–i* and Table 2) but not the ACC cluster. The insular clusters extended towards temporal lobe [Brodmann area (BA) 38] and inferior frontal cortex (BA 13/47) and were localized in anterior short gyrus and anterior inferior cortex within the bilateral insulae (Faillenot et al., 2017).

We further tested for significance of covariates (GLM 5). Except for the effect of Urgency on R1 in the cerebellum (cluster-$p = 0.001$), all other covariates were not significantly correlated (cluster-$p > 0.05$), thus not significantly increasing explained variance of models. The covariates also did not improve model fit when tested collectively (cluster-$p > 0.05$; GLM 6, 7), as such, we did not find significant effects of other addiction measures (e.g. CUDIT, DUDIT) on R1.

Prediction of AUDIT changes based on baseline R1

We then performed a machine-learning-based prediction of AUDIT changes after 2 years from baseline R1 patterns using relevance vector regression (RVR; Fig. 2). Even from the ROIs based on an independent anatomical atlas, the right insula revealed significant information in the R1 patterns for predicting AUDIT changes with Pearson correlation ($r \geqslant 0.2303$; $p \leqslant 0.035$), and root-mean-squared error (RMSE $\leqslant 3.59$; $p \leqslant 0.027$). However, the fit (R2) was not significantly better than random permutation (R2 < 0.054; $p \geqslant 0.299$) suggesting a large unexplained variance in the R1 patterns. The whole-brain model also significantly predicted AUDIT changes, but with a lower performance level than the insular and subcallosal cortex (Table 3).

Discussion

Using a data-driven approach, we show that greater R1, indexing grey matter myelination (Haast et al., 2016), in bilateral AIns and SCA predicts greater resilience to problematic alcohol use in youths from ages 15 to 26, a critical neurodevelopmental period. R1 was measured at baseline and alcohol misuse was measured using the AUDIT at baseline and 1- and 2-years follow-ups. These findings were specific to alcohol misuse controlled for age, gender, and impulsivity with no other structural relationships observed to other drug or behavioural addiction measures. We further corroborate these findings using machine learning, emphasizing the capacity to predict changes in alcohol resilience. Our hypothesis-free approach converges with a critical role for the AIns and SCA in disorders of addiction. Most strikingly, a recent longitudinal study also found an association of reduced growth of

Table 1. Descriptive statistics of demographic, impulsivity, and addictive behavioural variables and one-sample *t* test statistics for longitudinal changes of addictive behaviours

Variables	Min	Max	Mean	Std.	*T*-stat.	*p* val.
Age	15.75	26.67	21.76	2.76		
EP	1	4	2.36	1.20		
Urgency	26	72	43.92	10.81		
Premeditation	13	42	22.70	6.06		
Perseveration	10	29	17.41	4.46		
Sensation	19	46	32.53	6.39		
AUDIT(0)	0	29	8.76	5.95		
AUDIT(1)	0	28	8.43	5.60		
AUDIT(1–0)	−13	9	−0.33	3.39	−0.98	0.38
AUDIT(2)	0	23	7.62	4.76		
AUDIT(2–0)	−14	10	−1.14	3.63	−2.93	0.004
CUDIT(0)	0	25	2.80	5.27		
CUDIT(1)	0	22	1.73	4.46		
CUDIT(1–0)	−18	7	−1.07	3.38	−1.96	0.05
CUDIT(2)	0	25	2.36	5.53		
CUDIT(2–0)	−16	11	−0.44	3.46	−2.98	0.004
DUDIT(0)	0	23	1.48	4.04		
DUDIT(1)	0	17	0.84	3.33		
DUDIT(1–0)	−23	6	−0.64	3.00	0.98	0.33
DUDIT(2)	0	22	0.84	3.42		
DUDIT(2–0)	−23	4	−0.64	2.91	−1.87	0.06
IGD9(0)	0	45	9.98	9.16		
IGD9(1)	0	33	7.59	8.06		
IGD9(1–0)	−36	18	−2.38	7.42	−2.91	0.005
IGD9(2)	0	33	7.76	8.45		
IGD9(2–0)	−34	15	−2.22	7.01	−1.18	0.24
PCQ(0)	0	53	17.28	15.11		
PCQ(1)	0	78	18.63	17.50	−2.04	0.05
PCQ(1–0)	−50	44	1.35	12.75		
PCQ(2)	0	75	18.97	18.14	−2.94	0.004
PCQ(2–0)	−45	42	1.69	13.89		
BES(0)	0	20	7.34	4.75		
BES(1)	0	28	6.55	5.47		
BES(1–0)	−10	11	−0.79	3.91	1.13	0.26
BES(2)	8	25	12.34	3.52		
BES(2–0)	−8	14	5.00	3.90	11.90	$<10^{-18}$

AUDIT, Alcohol Use Disorder Identification Test; CUDIT, Cannabis Use Disorder Identification Test-Revised; DUDIT, Drug Use Disorder Identification Test; IGD, Internet Gaming Disorder Scale Short Format; PCQ, Pornography Craving Questionnaire; BES, Binge Eating Scale.
Note: Change from baseline is indicated by Δ. Urgency (combining positive and negative), premeditation, perseveration, and sensation (seeking) refer to the respective UPPS-P subscales. *p* values are uncorrected.

grey matter myelin in bilateral AIns with impulsivity in the adolescent population using a different technique (Ziegler et al., 2019). Previous functional research showed that the AIns is implicated in substance cue reactivity and craving in addiction disorders (Garavan, 2010; Naqvi & Bechara, 2010) and plays a role in predictive coding of autonomic function involving the comparison of actual and expected bodily/autonomic signals highly relevant to the subjective experience of cues and craving

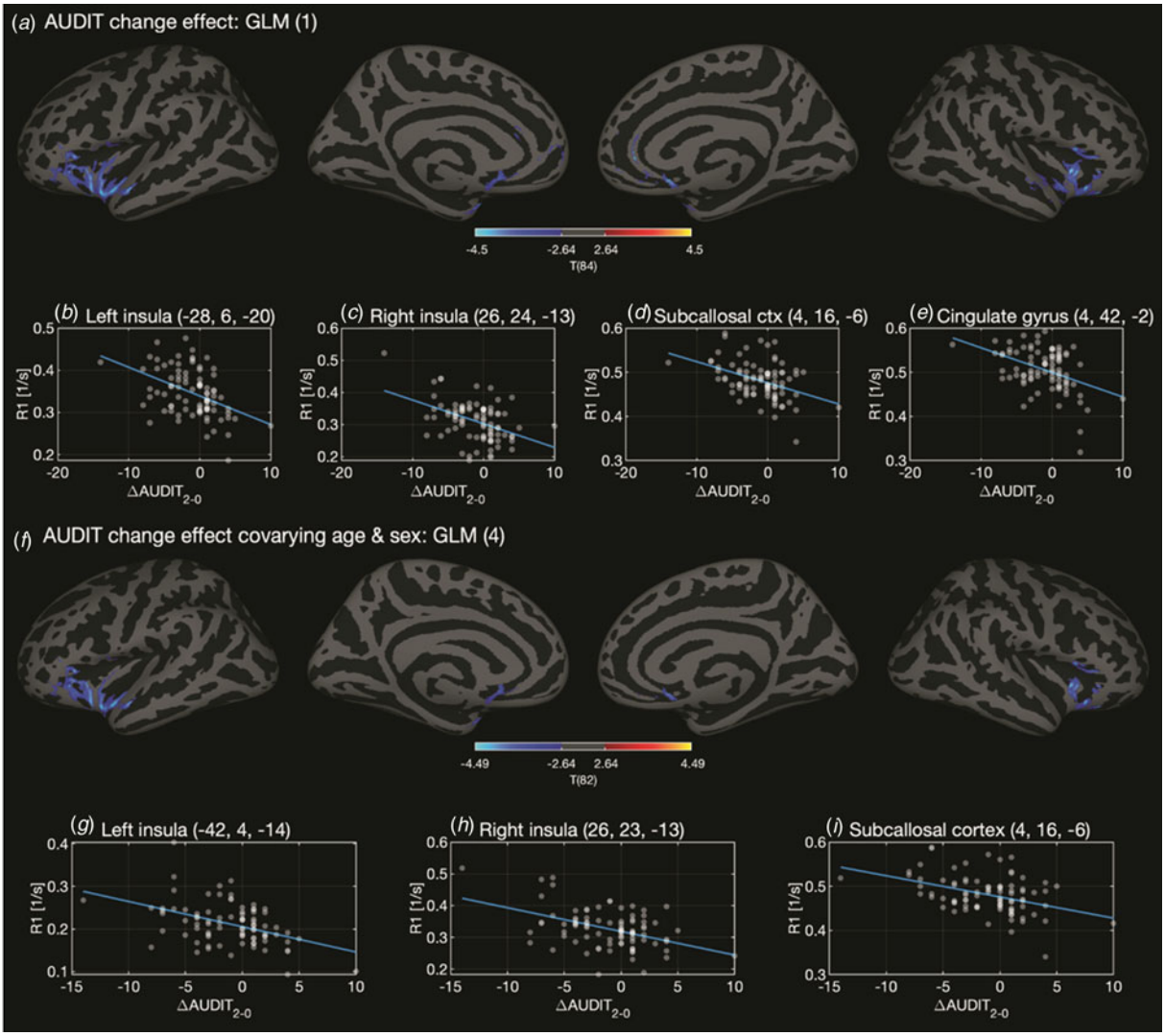

Fig. 1. Grey matter myeloarchitecture and prediction of problem alcohol behaviours. (*a*) *T*-statistic maps thresholded at the cluster-level *p* value of 0.05 testing the association between R1 and 2-year follow-up AUDIT changes without covariates. (*b–e*) Scatter plots and linear fits at peak voxels to illustrate the fitting. (*f*) *T*-statistic maps thresholded at the cluster-level *p* value of 0.05 testing the association between R1 and 2-year follow-up AUDIT changes with covariates of age and sex. (*g–i*) Scatter plots and linear fits at peak voxels. Surface visualization of results in volumetric space were done using FreeSurfer (https://surfer.nmr.mgh.harvard.edu/).

Table 2. Association between AUDIT changes and R1

					Peak MNI-coordinate			
Cluster location	BA	Max *Z*	Cluster-level *p*	Extent (voxel)	*X* (mm)	*Y* (mm)	*Z* (mm)	Adjusted R^2
(a) Effect of AUDIT change without covariates (GLM 1)								
Left insula	13/38/28	4.25	<0.001	2158	−28	6	−20	0.194
Right insula	13/22/47/13	4.23	<0.001	966	26	24	−13	0.193
Subcallosal cortex	25/34	3.92	<0.001	1113	4	16	−6	0.168
Anterior cingulate cortex	32/10/24	4.04	0.045	466	4	42	−2	0.177
(b) Effect of AUDIT change with age and sex covaried (GLM 4)								
Left insula	13/38	4.15	<0.001	1714	−42	4	−14	0.195
Right insula	13/47/45/13	4.20	0.020	539	26	23	−13	0.220
Subcallosal cortex	25/24	3.67	0.034	491	4	16	−6	0.179

AUDIT, Alcohol Use Disorder Identification Test; GLM, General Linear Model; BA, Broadman area.
Note: Cluster location was identified based on Harvard-Oxford Subcortical Atlas and Talairach Daemon Atlas in FSL (https://fsl.fmrib.ox.ac.uk/). Numerals of GLMs refer to in-text formulas.

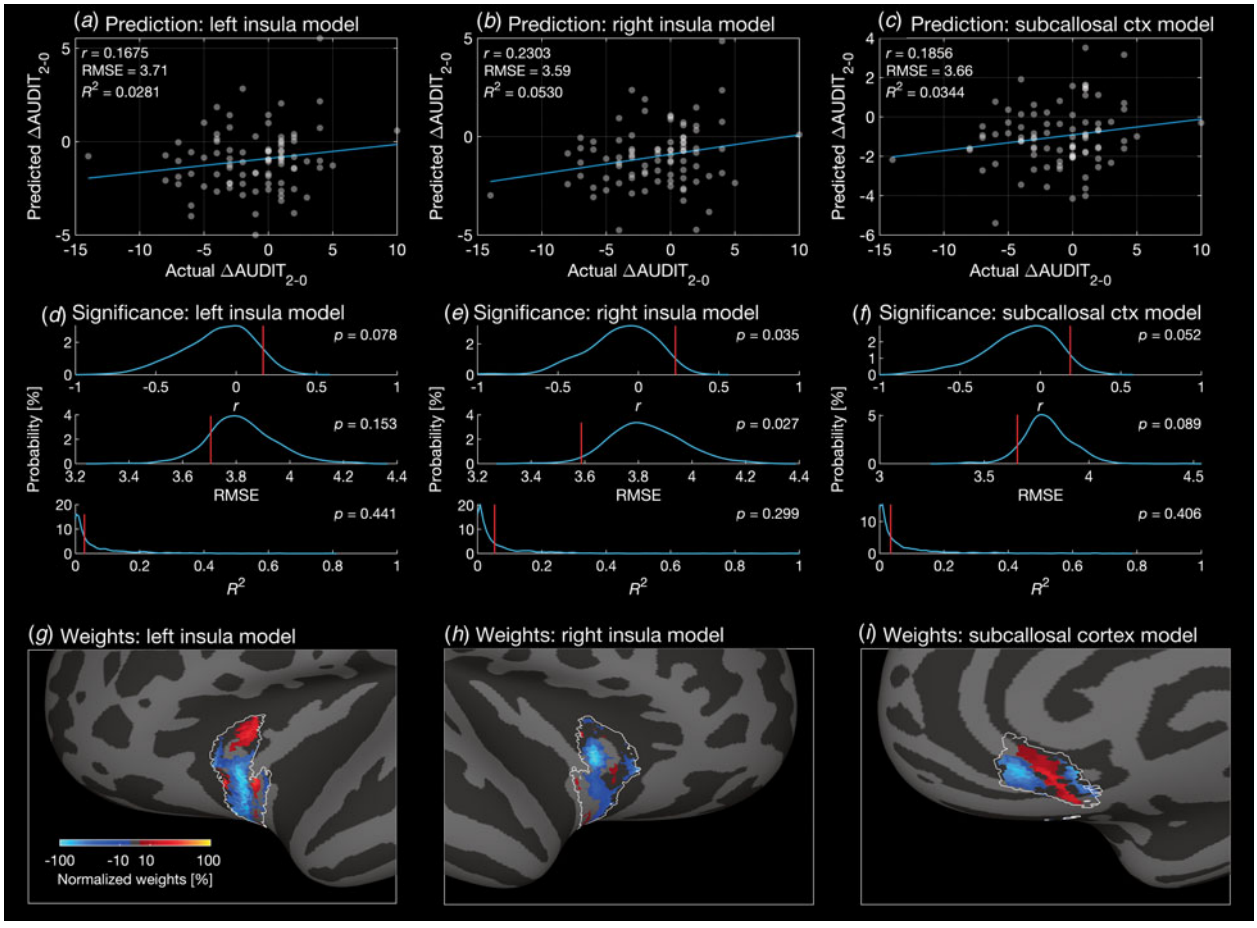

Fig. 2. R1 and prediction of problem alcohol behaviours using machine learning. (*a*–*c*) Scatter plot of prediction of AUDIT changes and actual AUDIT changes by relevant vector regression models based on R1 patterns in one of the anatomical regions of interest (*a*: left insula, *b*: right insula, *c*: subcallosal cortex). Performance measures [Pearson correlation coefficient, root-mean-squared error (RMSE), and R^2] are noted. (*d*–*f*) Significance of performance measures. Smoothed null distributions from random permutations of actual AUDIT changes are shown in blue and models' performances in red for each model. Non-parametric *p* values are noted. (*g*–*i*) Weights of each model are visualized on cortical surfaces, which are normalized by the maximum absolute weight and thresholded at 10% (anatomical regions of interest are outlined in white).

Table 3. Prediction of AUDIT changes based on baseline R1

Regions	*r*	*p* value (*r*)	RMSE	*p* value (RMSE)	R^2	*p* value (R^2)
Left insula	0.306	0.014	3.506	0.008	0.093	0.127
Right insula	0.464	0.001	3.244	0.001	0.216	0.077
Subcallosal cortex	0.363	0.005	3.371	0.004	0.132	0.207
All clusters	0.402	0.002	3.361	0.001	0.162	0.033
Whole-brain	0.279	0.010	3.482	0.012	0.078	0.060

AUDIT, Alcohol Use Disorder Identification Test; RVR, Relevant Vector Regression.
Note. *p* values were computed from 1000 permutations.

(Droutman, Read, & Bechara, 2015; Terasawa, Shibata, Moriguchi, & Umeda, 2013). Research on predictive markers in youth found greater neural activity to alcohol cues in the insula (Dager et al., 2014), similarly, greater reward-related activity in the insular cortex predicted early onset of alcohol consumption in 14-year olds (Nees et al., 2012). The AIns is also implicated in risk representation (Preuschoff, Bossaerts, & Quartz, 2006) and decision-making involving risk-taking (Xue, Lu, Levin, & Bechara, 2010), processes highly relevant to alcohol misuse (Preuschoff, Quartz, & Bossaerts, 2008; Rogers et al., 1999). For example, the continued use of substances despite the likelihood of adverse effects involves the evaluation of risk (Rogers et al., 1999) and risk-taking behaviour predicts drinking problems in undergraduates (Fernie, Cole, Goudie, & Field, 2010). The AIns signals risk prediction and risk prediction error (Preuschoff et al., 2008), and suboptimal computation of risk has been

shown in substance abusers (Gowin, Mackey, & Paulus, 2013). In addition to the insula, the SCA expressed a negative relationship to alcohol intake over time, the SCA is a critical node underlying emotional regulation (Mayberg et al., 1999; Phan, Wager, Taylor, & Liberzon, 2002) and its significance in predicting AUDIT change highlights its role in negative emotionality theories in addiction (Kwako, Momenan, Litten, Koob, & Goldman, 2016). The dorsal cingulate, a region implicated in substance cue reactivity and craving, also showed a relationship with resilience but was no longer significant after covarying for age and gender, highlighting the importance of demographic variables for prospective alcohol usage.

Of note, the current sample expressed a general reduction from baseline scores on addiction questionnaires over the 2-year period, which converges with earlier reports on age-related reductions in impulsive and addictive behaviours across maturity stages (Bachman, Wadsworth, O'Malley, Johnston, & Schulenberg, 2013). While the available data are not sufficient to assess changes in impulsivity levels longitudinally, early research indicates that an important impulsivity trait for the initiation of substance use, sensation seeking, peaks during late adolescence and declines thereafter (Zuckerman, 1994). Similarly, alcohol and drug use peaks between 20 and 24 years (World Health Organization, 2018) and declines thereafter (Arnett, 2000; Chassin, Flora, & King, 2004; Chen & Kandel, 1995) with problem drinking usually maturing out before the age of 28 (Bennett, McCrady, Johnson, & Pandina, 1999). Given that maturity as well as changes in impulsive behaviours, such as alcohol consumption, evolve gradually (Arnett, 2000; Chassin et al., 2004; Chen & Kandel, 1995), this might explain the lack of significant correlations between R1 and 1-year AUDIT change. At the 1-year follow-up, the marginally negative change in AUDIT scores did not significantly relate to impulsivity, whereas strong negative correlations were present at the 2-year follow-up. Similarly, the change in AUDIT scores between baseline and 1-year follow-up was not significant. We, therefore, conclude that a 1-year follow-up was not sufficient for expressing a significant change in drinking behaviour, which restricted the range of AUDIT change scores at 1-year post-baseline and therefore reduced the chance to detect significant correlations with R1.

Other structural changes than grey matter myelination

To investigate whether the current findings are specific to R1 in the grey matter or reflect general predictive abilities of measures of structural integrity, we assessed GMV and FA in addition to baseline R1. However, no significant relationship between the AUDIT or other addiction measures and other structural measures emerged. GMV and FA capture different properties of grey matter: GMV is an aggregative measure reflecting various morphological characteristics including mesoscopic geometry (Mechelli, Price, Friston, & Ashburner, 2005). Cortical FA likely reflects the complexity of (unmyelinated) dendrites, which are abundant in the cortex, rather than myelinated axons, which are fewer in the cortex as supported by animal models (Huang, Yamamoto, Hossain, Younes, & Mori, 2008). In contrast, R1 is sensitive to myelination density in grey matter irrespective of orientation. Thus, R1 provides unique quantification of local connectivity of microcircuits in grey matter, which is not captured by GMV and FA. Our findings therefore highlight not only which brain areas are predictive of subsequent changes in alcohol consumption, but additionally the utility of R1 in detecting important biomarkers above more commonly used structural measures such as GMV and FA.

Anterior insula and alcohol misuse

Our main finding relates to the predictive properties of insular R1 for subsequent alcohol usage. The AIns is critical for various addictions and addiction-related processes, e.g. human insular stroke lesions decrease nicotine dependence and craving symptoms (Naqvi, Rudrauf, Damasio, & Bechara, 2007). In response to alcohol cues, alcohol-dependent patients express higher insular activity (Dager et al., 2014; Myrick et al., 2004) and young adults in the SCA (Tapert, Brown, Baratta, & Brown, 2004). Across a range of drug and alcohol cues, some meta-analyses implicate greater cue reactivity in the AIns (Engelmann et al., 2012; Schacht, Anton, & Myrick, 2013; But see Chase, Eickhoff, Laird, & Hogarth, 2011). Enhanced left insular alcohol cue reactivity was also predictive for transitioning from moderate to heavy alcohol consumption in college students (Dager et al., 2014).

In addition to functional abnormalities in this brain area, structural insular abnormalities have also been reported with problematic alcohol misuse. White matter integrity, as indicated by FA, in the right insula correlates positively with craving in adolescents seeking treatment for substance abuse (Chung & Clark, 2014). Lower AIns GMV has also been reported in alcohol-dependent patients relative to controls (Senatorov et al., 2015). With alcohol abstinence, both insular and cingulate increase their GMV within a 3-month period compared to non-abstinence (Demirakca et al., 2011). The AIns is also implicated across a range of substance use disorders in cross-sectional studies. Lower GMV in the right insula has been reported in heroin and cocaine (Gardini & Venneri, 2012), methamphetamine (Schwartz et al., 2010) and nicotine dependence (Stoeckel, Chai, Zhang, Whitfield-Gabrieli, & Evins, 2016). GMV in both the AIns and SCA correlate with years of cocaine use (Connolly, Bell, Foxe, & Garavan, 2013). Here, no cross-sectional relationships between structural measures and baseline addiction measures were found, potentially due to the healthy sample and to excluding participants with addiction disorders at baseline, but this also suggests that our findings were unrelated to the effects of alcohol misuse itself.

Insular findings were localized to the ventral part of the AIns, a region specifically implicated in substance cue reactivity and craving (Butti, Santos, Uppal, & Hof, 2013; Franklin et al., 2007; Venniro et al., 2017). Relapse to methamphetamine in rodents is associated with selective activation of a glutamatergic pathway relaying information from the ventral AIns to the central amygdala and chemogenetic inhibition of this projection decreased relapse (Venniro et al., 2017). Furthermore, human AIns post-mortem studies indicate a 60% reduction in Von Economo neurons (VENs) in those with alcohol use disorders and corresponding volumetric reductions (Senatorov et al., 2015). VENs are also common in the ACC (Butti et al., 2013), which showed a significant relationship between R1 and change in alcohol consumption, but was no longer significant when controlling for age and gender.

Limitations

A relative wide age range (15.8–26.7 years) was employed and as such participants were likely in different maturity stages. We accounted for this by using age as a covariate, but the term

adolescents/young adults should be seen in relation to the studied age range. Further, R1 was only assessed at baseline. Although we did not find cross-sectional relationships between R1 and the degree of problem alcohol use, whether R1 changes with alcohol consumption is undetermined. We anticipated a greater number of subjects would increase problem drinking given the stratification by EP. As common for prospective studies (e.g. IMAGEN; Schumann et al., 2010), participants with pre-existing substance abuse problems were excluded to enable prediction of future alcohol misuse and resilience to it, independently of pre-existing conditions that might have had neural consequences. This might have reduced the range of AUDIT scores at baseline and precluded the ability to investigate whether increased myelination acts as resilience factor in those with a history of substance abuse. Non-significant correlations between GMV, FA and AUDIT scores might relate to the age range and the low alcohol usage in this sample; Structural abnormalities due to excessive alcohol consumption, such as reduced GMV in the insula and reduced global cortical thickness (Momenan et al., 2012) have not yet taken place in this population.

For technical considerations, R1 is not only sensitive to myelin but also iron content. An *ex vivo* study showed enhanced contribution of myelin over iron (Stüber et al., 2014), but the interpretation of *in vivo* R1 should be still cautious. There are other MR images that have been used to characterize myeloarchitecture as well. A ratio of T1-weighted signal over T2-weighted signal (i.e. T1w/T2w) has been widely used for its availability (Glasser & Van Essen, 2011). MT imaging is a semi-quantitative (as the MT ratio is dependent on a flip angle) technique based on cross-relaxation between protons in macromolecules such as lipids in myelin (Helms, Dathe, Kallenberg, & Dechent, 2008). Quantitative magnetization susceptibility mapping (QSM) also has demonstrated its high agreement to known cytoarchitecture (Deistung et al., 2013) for its sensitivity to iron (Langkammer et al., 2012). In addition, T2* mapping also showed a good agreement with known myelo-/cytoarchitecture of the human cerebral cortex for its sensitivity to both myelin and iron (Govindarajan et al., 2015). In fact, a comparison among R1, R2* (= 1/T2*), and QSM at a high resolution (0.65-mm isotropic) revealed that both R1 and R2* are suitable for myelo-/cytoarchitecture parcellation but QSM showed more complex behaviours (Marques, Khabipova, & Gruetter, 2017). For their different sensitivity and selectivity to different macromolecules, use of multiple quantitative mapping [R1, effective proton density (PD*), MT, R2*] has been proposed to acquire comprehensive quantitative imaging that can better differentiate myelin and iron (Weiskopf et al., 2013).

Conclusions

In sum, we show using a data-driven approach that R1, indexing cortical myelination, can predict future resilience to problematic alcohol behaviours in youths in key regions underlying disorders of addiction. Our findings have high clinical relevance for problematic alcohol use since the early age of alcohol use predicts subsequent misuse (World Health Organization, 2018). The current sample largely decreased their alcohol usage over time and as such, we were able to identify that increased myelination in the AIns predicts this decline in alcohol usage. Theories of alcohol addiction commonly do not account for neural factors predating alcohol usage, despite their ability to shed light on the neural underpinning determining the trajectories from habitual to problematic alcohol usage independent of pre-existing alcohol-related neural alterations. AIns myelination may represent a specific biomarker of potential alcohol resilience for early identification and intervention studies. It can be assumed that targeting the at-risk youths with intervention programmes at an early age might prevent future worsening of the condition and associated health problems. However, the majority of currently available treatment options are medication-based (e.g. Witkiewitz, Litten, and Leggio, 2019), while early prevention programmes targeting at-risk youth might benefit from applying non-pharmacological, psychological treatments aimed at motivation and self-control which have been shown to be similarly effective (Imel, Wampold, Miller, & Fleming, 2008). Further large-scale studies to assess the utility of R1 as a biomarker in both youths and adults or as a predictor of treatment outcome and potential means of modifying grey matter myeloarchitecture as a potential treatment target are indicated.

Supplementary material. The supplementary material for this article can be found at https://doi.org/10.1017/S0033291720003852

Acknowledgements. The authors would like to thank the participants for taking time to travel to Aarhus and take part in the study, and Michael Mulbjerg Pedersen (Aarhus University), Timo Lehman Kvamme (Aarhus University), Nuria Donamayor (University of Cambridge), Kwangyeol Baek (University of Cambridge), and Daisy Mechelmans (University of Cambridge) for helping with the data collection, and Center of Functionally Integrative Neuroscience/MINDLab for use of their great facilities. VV is funded on a Medical Research Council Senior Fellowship (MR/P008747/1). MBC, KRT and MUP are funded by the Danish Ministry for Social Affairs and the Interior (9173-0003). The study was supported by Aarhus University Research Foundation (AUFF), Assistant Professor Starting Grant (R46-A4016: KRT, MBC, MUP, VV).

Conflict of interest. None.

Ethical standards. The authors assert that all procedures contributing to this work comply with the ethical standards of the relevant national and institutional committees on human experimentation and with the Helsinki Declaration of 1975, as revised in 2008.

References

Adamson, S. J., & Sellman, J. D. (2003). A prototype screening instrument for cannabis use disorder: The Cannabis Use Disorders Identification Test (CUDIT) in an alcohol-dependent clinical sample. *Drug and Alcohol Review*, *22*, 309–315.

Allen, M., Frank, D., Glen, J. C., Fardo, F., Callaghan, M. F., & Rees, G. (2017). Insula and somatosensory cortical myelination and iron markers underlie individual differences in empathy. *Scientific Reports*, *7*, 43316.

Arnett, J. J. (2000). Emerging adulthood: A theory of development from the late teens through the twenties. *American Psychologist*, *55*, 469–480.

Ashburner, J., & Friston, K. J. (2000). Voxel-based morphometry - the methods. *NeuroImage*, *11*, 805–821.

Ashburner, J., & Friston, K. J. (2005). Unified segmentation. *NeuroImage*, *26*, 839–851.

Bachman, J. G., Wadsworth, K. N., O'Malley, P. M., Johnston, L. D., & Schulenberg, J. E. (2013). *Smoking, drinking, and drug use in young adulthood: The impacts of new freedoms and new responsibilities*. Mahwah, NJ: Psychology Press.

Ballman, K. V. (2015). Biomarker: Predictive or prognostic? *Journal of Clinical Oncology: Official Journal of the American Society of Clinical Oncology*, *33*, 3968–3971.

Basser, P. J., Mattiello, J., & LeBihan, D. (1994). MR Diffusion tensor spectroscopy and imaging. *Biophysical Journal*, *66*, 259–267.

Behrendt, S., Wittchen, H.-U., Höfler, M., Lieb, R., & Beesdo, K. (2009). Transitions from first substance use to substance use disorders in

adolescence: Is early onset associated with a rapid escalation? *Drug and Alcohol Dependence*, *99*, 68–78.
Bennett, M. E., McCrady, B. S., Johnson, V., & Pandina, R. J. (1999). Problem drinking from young adulthood to adulthood: Patterns, predictors and outcomes. *Journal of Studies on Alcohol*, *60*, 605–614.
Berman, A. H., Bergman, H., Palmstierna, T., & Schlyter, F. (2005). Evaluation of the Drug Use Disorders Identification Test (DUDIT) in criminal justice and detoxification settings and in a Swedish population sample. *European Addiction Research*, *11*, 22–31.
Butti, C., Santos, M., Uppal, N., & Hof, P. R. (2013). Von Economo neurons: Clinical and evolutionary perspectives. *Cortex*, *491*, 312–326.
Callaghan, M. F., Freund, P., Draganski, B., Anderson, E., Cappelletti, M., Chowdhury, R., … Weiskopf, N. (2014). Widespread age-related differences in the human brain microstructure revealed by quantitative magnetic resonance imaging. *Neurobiology of Aging*, *35*, 1862–1872.
Chase, H. W., Eickhoff, S. B., Laird, A. R., & Hogarth, L. (2011). The neural basis of drug stimulus processing and craving: An activation likelihood estimation meta-analysis. *Biological Psychiatry*, *70*, 785–793.
Chassin, L., Flora, D. B., & King, K. M. (2004). Trajectories of alcohol and drug use and dependence from adolescence to adulthood: The effects of familial alcoholism and personality. *Journal of Abnormal Psychology*, *113*, 483–498.
Chen, K., & Kandel, D. B. (1995). The natural history of drug use from adolescence to the mid-thirties in a general population sample. *American Journal of Public Health*, *85*, 41–47.
Chung, T., & Clark, D. B. (2014). Insula white matter volume linked to binge drinking frequency through enhancement motives in treated adolescents. *Alcoholism: Clinical and Experimental Research*, *38*, 1932–1940.
Connolly, C. G., Bell, R. P., Foxe, J. J., & Garavan, H. (2013). Dissociated grey matter changes with prolonged addiction and extended abstinence in cocaine users. *PLoS One*, *8*, e59645.
Cyders, M. A., Smith, G. T., Spillane, N. S., Fischer, S., Annus, A. M., & Peterson, C. (2007). Integration of impulsivity and positive mood to predict risky behavior: Development and validation of a measure of positive urgency. *Psychological Assessment*, *19*, 107–118.
Dager, A. D., Anderson, B. M., Rosen, R., Khadka, S., Sawyer, B., Jiantonio-Kelly, R. E., … Pearlson, G. D. (2014). Functional magnetic resonance imaging (fMRI) response to alcohol pictures predicts subsequent transition to heavy drinking in college students. *Addiction*, *109*, 585–595.
Deistung, A., Schäfer, A., Schweser, F., Biedermann, U., Turner, R., & Reichenbach, J. R. (2013). Toward in vivo histology: A comparison of quantitative susceptibility mapping (QSM) with magnitude-, phase-, and R2*-imaging at ultra-high magnetic field strength. *NeuroImage*, *65*, 299–314.
Demirakca, T., Ende, G., Kammerer, N., Welzel-Marquez, H., Hermann, D., Heinz, A., & Mann, K. (2011). Effects of alcoholism and continued abstinence on brain volumes in both genders. *Alcoholism: Clinical and Experimental Research*, *35*, 1678–1685.
Droutman, V., Read, S. J., & Bechara, A. (2015). Revisiting the role of the insula in addiction. *Trends in Cognitive Sciences*, *19*, 414–420.
Edwards, L. J., Kirilina, E., Mohammadi, S., & Weiskopf, N. (2018). Microstructural imaging of human neocortex in vivo. *NeuroImage*, *182*, 184–206.
Engelmann, J. M., Versace, F., Robinson, J. D., Minnix, J. A., Lam, C. Y., Cui, Y., … Cinciripini, P. M. (2012). Neural substrates of smoking cue reactivity: A meta-analysis of fMRI studies. *NeuroImage*, *60*, 252–262.
Faillenot, I., Heckemann, R. A., Frot, M., & Hammers, A. (2017). Macroanatomy and 3D probabilistic atlas of the human insula. *NeuroImage*, *150*, 88–98.
Fernie, G., Cole, J. C., Goudie, A. J., & Field, M. (2010). Risk-taking but not response inhibition or delay discounting predict alcohol consumption in social drinkers. *Drug and Alcohol Dependence*, *112*, 54–61.
Franklin, T. R., Wang, J., Sciortino, N., Harper, D., Li, Y., Ehrman, R., … Childress, A. R. (2007). Limbic activation to cigarette smoking cues independent of nicotine withdrawal: A perfusion fMRI study. *Neuropsychopharmacology*, *32*, 2301–2309.
Garavan, H. (2010). Insula and drug cravings. *Brain Structure and Function*, *214*, 593–601.
Gardini, S., & Venneri, A. (2012). Reduced grey matter in the posterior insula as a structural vulnerability or diathesis to addiction. *Brain Research Bulletin*, *87*, 205–211.
Glasser, M. F., & Van Essen, D. C. (2011). Mapping human cortical areas in vivo based on myelin content as revealed by T1- and T2-weighted MRI. *Journal of Neuroscience*, *31*, 11597–11616.
Gormally, J., Black, S., Daston, S., & Rardin, D. (1982). The assessment of binge eating severity among obese persons. *Addictive Behaviors*, *7*, 47–55.
Govindarajan, S. T., Cohen-Adad, J., Sormani, M. P., Fan, A. P., Louapre, C., & Mainero, C. (2015). Reproducibility of T2* mapping in the human cerebral cortex in vivo at 7 tesla MRI. *Journal of Magnetic Resonance Imaging*, *42*, 290–296.
Gowin, J. L., Mackey, S., & Paulus, M. P. (2013). Altered risk-related processing in substance users: Imbalance of pain and gain. *Drug and Alcohol Dependence*, *132*, 13–21.
Haast, R. A., Ivanov, D., Formisano, E., & Uludag, K. (2016). Reproducibility and reliability of quantitative and weighted T1 and T2(*) mapping for myelin-based cortical parcellation at 7 tesla. *Frontiers in Neuroanatomy*, *10*, 112.
Hawkins, J. D., Catalano, R. F., & Miller, J. Y. (1992). Risk and protective factors for alcohol and other drug problems in adolescence and early adulthood: Implications for substance abuse prevention. *Psychological Bulletin*, *112*, 64–105.
Helms, G., Dathe, H., Kallenberg, K., & Dechent, P. (2008). High-resolution maps of magnetization transfer with inherent correction for RF inhomogeneity and T1 relaxation obtained from 3D FLASH MRI. *Magnetic Resonance in Medicine*, *60*, 1396–1407.
Hodder, R. K., Campbell, E., Gilligan, C., Lee, H., Lecathelinais, C., Green, S., … Wiggers, J. (2018). Association between Australian adolescent alcohol use and alcohol use risk and protective factors in 2011 and 2014. *Drug and Alcohol Review*, *37*, S22–S33.
Huang, H., Yamamoto, A., Hossain, M. A., Younes, L., & Mori, S. (2008). Quantitative cortical mapping of fractional anisotropy in developing rat brains. *Journal of Neuroscience*, *28*, 1427–1433.
Imel, Z. E., Wampold, B. E., Miller, S. D., & Fleming, R. R. (2008). Distinctions without a difference: Direct comparisons of psychotherapies for alcohol use disorders. *Psychology of Addictive Behaviors*, *22*, 533–543.
Keuken, M., Bazin P-L, B., K., Beekhuizen, S., Himmer, L., Kandola, A., Lafeber, J. J., … Turner, R. (2017). Effects of aging on T1, T2*, and QSM MRI values in the subcortex. *Brain Structure and Function*, *222*, 2487–2505.
Kim, S. G., & Knoesche, T. R. (2016). Intracortical myelination in musicians with absolute pitch: Quantitative morphometry using 7-T MRI. *Human Brain Mapping*, *37*, 3486–3501.
Kraus, S., & Rosenberg, H. (2014). The pornography craving questionnaire: Psychometric properties. *Archives of Sexual Behavior*, *43*, 451–462.
Kriegeskorte, N., Simmons, W. K., Bellgowan, P. S., & Baker, C. I. (2009). Circular analysis in systems neuroscience: The dangers of double dipping. *Nature Neuroscience*, *12*, 535–540.
Kwako, L. E., Momenan, R., Litten, R. Z., Koob, G. F., & Goldman, D. (2016). Addictions neuroclinical assessment: A neuroscience-based framework for addictive disorders. *Biological Psychiatry*, *80*, 179–189.
Langkammer, C., Schweser, F., Krebs, N., Deistung, A., Goessler, W., Scheurer, E., … Reichenbach, J. R. (2012). Quantitative susceptibility mapping (QSM) as a means to measure brain iron? A post mortem validation study. *NeuroImage*, *62*, 1593–1599.
Lynam, D. R., Smith, G. T., Whiteside, S. P., & Cyders, M. A. (2006). *The UPPS-P: Assessing five personality pathways to impulsive behavior*. West Lafayette, IN: Purdue University.
Marques, J. P., Khabipova, D., & Gruetter, R. (2017). Studying cyto and myeloarchitecture of the human cortex at ultra-high field with quantitative imaging: R1, R2* and magnetic susceptibility. *NeuroImage*, *147*, 152–163.
Marques, J. P., Kober, T., Krueger, G., van der Zwaag, W., Van de Moortele, P.-F., & Gruetter, R. (2010). MP2RAGE, A self bias-field corrected sequence for improved segmentation and T1-mapping at high field. *NeuroImage*, *49*, 1271–1281.

Mayberg, H. S., Liotti, M., Brannan, S. K., McGinnis, S., Mahurin, R. K., Jerabek, P. A., & Lancaster, J. L. (1999). Reciprocal limbic-cortical function and negative mood: Converging PET findings in depression and normal sadness. *American Journal of Psychiatry*, *156*, 675–682.

Mechelli, A., Price, C. J., Friston, K. J., & Ashburner, J. (2005). Voxel-based morphometry of the human brain: Methods and applications. *Current Medical Imaging*, *1*, 105–113.

Momenan, R., Steckler, L. E., Saad, Z. S., van Rafelghem, S., Kerich, M. J., & Hommer, D. W. (2012). Effects of alcohol dependence on cortical thickness as determined by magnetic resonance imaging. *Psychiatry Research*, *204*, 101–111.

Myrick, H., Anton, R. F., Li, X., Henderson, S., Drobes, D., Voronin, K., & George, M. S. (2004). Differential brain activity in alcoholics and social drinkers to alcohol cues: Relationship to craving. *Neuropsychopharmacology*, *29*, 393–402.

Naqvi, N. H., & Bechara, A. (2010). The insula and drug addiction: An interoceptive view of pleasure, urges, and decision-making. *Brain Structure and Function*, *214*, 435–450.

Naqvi, N. H., Rudrauf, D., Damasio, H., & Bechara, A. (2007). Damage to the insula disrupts addiction to cigarette smoking. *Science (New York, N.Y.)*, *315*, 531–534.

Nees, F., Tzschoppe, J., Patrick, C. J., Vollstadt-Klein, S., Steiner, S., Poustka, L., … Flor, H. (2012). Determinants of early alcohol use in healthy adolescents: The differential contribution of neuroimaging and psychological factors. *Neuropsychopharmacology*, *37*, 986–995.

Nord, C. L., Kim, S.-G., Callesen, M. B., Kvamme, T. L., Jensen, M., Pedersen, M. U., & Voon, V. (2019). The myeloarchitecture of impulsivity: Premature responding in youth is associated with decreased myelination of ventral putamen. *Neuropsychopharmacology*, *44*, 1216–1223.

Pedersen, M. U., Rømer Thomsen, K., Pedersen, M. M., & Hesse, M. (2017). Mapping risk factors for substance use: Introducing the YouthMap12. *Addictive Behaviors*, *65*, 40–50.

Phan, K. L., Wager, T., Taylor, S. F., & Liberzon, I. (2002). Functional neuroanatomy of emotion: A meta-analysis of emotion activation studies in PET and fMRI. *NeuroImage*, *16*, 331–348.

Pontes, H. M., & Griffiths, M. D. (2015). Measuring DSM-5 Internet gaming disorder: Development and validation of a short psychometric scale. *Computers in Human Behavior*, *45*, 137–143.

Preuschoff, K., Bossaerts, P., & Quartz, S. R. (2006). Neural differentiation of expected reward and risk in human subcortical structures. *Neuron*, *51*, 381–390.

Preuschoff, K., Quartz, S. R., & Bossaerts, P. (2008). Human insula activation reflects risk prediction errors as well as risk. *Journal of Neuroscience*, *28*, 2745–2752.

Rogers, R. D., Everitt, B., Baldacchino, A., Blackshaw, A., Swainson, R., Wynne, K., … Booker, E. (1999). Dissociable deficits in the decision-making cognition of chronic amphetamine abusers, opiate abusers, patients with focal damage to prefrontal cortex, and tryptophan-depleted normal volunteers: Evidence for monoaminergic mechanisms. *Neuropsychopharmacology*, *20*, 322–339.

Rømer Thomsen, K., Callesen, M. B., Hesse, M., Kvamme, T. L., Pedersen, M. M., Pedersen, M. U., & Voon, V. (2018). Impulsivity traits and addiction-related behaviors in youth. *Journal of Behavioral Addictions*, *7*, 317–330.

Rømer Thomsen, K., Joensson, M., Lou, H. C., Møller, A., Gross, J., Kringelbach, M. L., & Changeux, J.-P. (2013). Altered paralimbic interaction in behavioral addiction. *Proceedings of the National Academy of Sciences*, *110*, 4744–4749.

Rooney, W. D., Johnson, G., Li, X., Cohen, E. R., Kim, S. G., Ugurbil, K., & Springer Jr, C. S. (2007). Magnetic field and tissue dependencies of human brain longitudinal 1H2O relaxation in vivo. *Magnetic Resonance in Medicine: An Official Journal of the International Society for Magnetic Resonance in Medicine*, *57*, 308–318.

Sacchet, M. D., & Gotlib, I. H. (2017). Myelination of the brain in Major Depressive Disorder: An in vivo quantitative magnetic resonance imaging study. *Scientific Reports*, *7*, 2200.

Saunders, J. B., Aasland, O. G., Babor, T. F., De la Fuente, J. R., & Grant, M. (1993). Development of the alcohol use disorders identification test (AUDIT): WHO collaborative project on early detection of persons with harmful alcohol consumption-II. *Addiction*, *88*, 791–804.

Schacht, J. P., Anton, R. F., & Myrick, H. (2013). Functional neuroimaging studies of alcohol cue reactivity: A quantitative meta-analysis and systematic review. *Addiction Biology*, *18*, 121–133.

Scheier, L. M., Botvin, G. J., & Baker, E. (1997). Risk and protective factors as predictors of adolescent alcohol involvement and transitions in alcohol use: A prospective analysis. *Journal of Studies on Alcohol*, *58*, 652–667.

Schrouff, J., Rosa, M. J., Rondina, J. M., Marquand, A. F., Chu, C., Ashburner, J., … Mourão-Miranda, J. (2013). PRoNTo: Pattern recognition for neuroimaging toolbox. *Neuroinformatics*, *11*, 319–337.

Schumann, G., Loth, E., Banaschewski, T., Barbot, A., Barker, G., Büchel, C., … Gallinat, J. (2010). The IMAGEN study: Reinforcement-related behaviour in normal brain function and psychopathology. *Molecular Psychiatry*, *15*, 1128–1139.

Schwartz, D. L., Mitchell, A. D., Lahna, D. L., Luber, H. S., Huckans, M. S., Mitchell, S. H., & Hoffman, W. F. (2010). Global and local morphometric differences in recently abstinent methamphetamine-dependent individuals. *NeuroImage*, *50*, 1392–1401.

Senatorov, V. V., Damadzic, R., Mann, C. L., Schwandt, M. L., George, D. T., Hommer, D. W., … Momenan, R. (2015). Reduced anterior insula, enlarged amygdala in alcoholism and associated depleted von Economo neurons. *Brain*, *138*, 69–79.

Seo, S, Beck, A, Matthis, C, Genauck, A, Banaschewski, T, Bokde, A, … Frouin, V. (2019). Risk profiles for heavy drinking in adolescence: differential effects of gender. *Addiction biology*, *24*(4), 787–801.

Seo, S, Mohr, J, Beck, A, Wüstenberg, T, Heinz, A, & Obermayer, K. (2015). Predicting the future relapse of alcohol-dependent patients from structural and functional brain images. *Addiction biology*, *20*(6), 1042–1055.

Stoeckel, L. E., Chai, X. J., Zhang, J., Whitfield-Gabrieli, S., & Evins, A. E. (2016). Lower gray matter density and functional connectivity in the anterior insula in smokers compared with never smokers. *Addiction Biology*, *21*, 972–981.

Stüber, C., Morawski, M., Schäfer, A., Labadie, C., Wähnert, M., Leuze, C., … Geyer, S. (2014). Myelin and iron concentration in the human brain: A quantitative study of MRI contrast. *NeuroImage*, *93*, 95–106.

Tapert, S. F., Brown, G. G., Baratta, M. V., & Brown, S. A. (2004). fMRI BOLD response to alcohol stimuli in alcohol dependent young women. *Addictive Behaviors*, *29*, 33–50.

Terasawa, Y., Shibata, M., Moriguchi, Y., & Umeda, S. (2013). Anterior insular cortex mediates bodily sensibility and social anxiety. *Social Cognitive and Affective Neuroscience*, *8*, 259–266.

Tipping, M. E. (2001). Sparse Bayesian learning and the relevance vector machine. *Journal of Machine Learning Research*, *1*, 211–244.

Venniro, M., Caprioli, D., Zhang, M., Whitaker, L. R., Zhang, S., Warren, B. L., … Shaham, Y. (2017). The anterior insular cortex-->central amygdala glutamatergic pathway Is critical to relapse after contingency management. *Neuron*, *96*, 414–427 e8.

Weiskopf, N., Suckling, J., Williams, G., Correia, M., Inkster, B., Tait, R., … Lutti, A. (2013). Quantitative multi-parameter mapping of R1, PD*, MT, and R2* at 3T: A multi-center validation. *Frontiers in Neuroscience*, *7*, 95.

Whelan, R., Watts, R., Orr, C. A., Althoff, R. R., Artiges, E., Banaschewski, T., … Garavan, H. (2014). Neuropsychosocial profiles of current and future adolescent alcohol misusers. *Nature*, *512*, 185–189.

Witkiewitz, K., Litten, R., & Leggio, L. (2019). Advances in the science and treatment of alcohol use disorder. *Science Advances*, *5*, eaax4043.

World Health Organization (2018). Global status report on alcohol and health. Retrieved from https://apps.who.int/iris/bitstream/handle/10665/274603/9789241565639-eng.pdf?ua=1.

Worsley, K. J., Evans, A. C., Marrett, S., & Neelin, P. (1992). A three-dimensional statistical analysis for CBF activation studies in human brain. *Journal of Cerebral Blood Flow & Metabolism*, *12*, 900–918.

Xue, G., Lu, Z., Levin, I. P., & Bechara, A. (2010). The impact of prior risk experiences on subsequent risky decision-making: The role of the insula. *NeuroImage*, *50*, 709–716.

Ziegler, G., Hauser, T. U., Moutoussis, M., Bullmore, E. T., Goodyer, I. M., Fonagy, P., … Dolan, R. J. (2019). Compulsivity and impulsivity traits linked to attenuated developmental frontostriatal myelination trajectories. *Nature Neuroscience*, *22*, 992–999.

Zuckerman, M. (1994). *Behavioral expressions and biosocial bases of sensation seeking*. Cambridge: Cambridge university press.